Electronics, Communications and Networks
A.J. Tallón-Ballesteros et al. (Eds.)

doi:10.3233/FAIA231189

PID Frequency Tracking Method of Electrodynamic Exciter Based on Resonant Effects

Shengshuan JIAO, Wentao LIU[1], Jiafeng WU, Shouren WANG and Tiantian LI
School of Mechanical Engineering, University of Jinan, Jinan 250022, China

Abstract. A new type of electrodynamic exciter was proposed based on resonant effects in this paper. A PID frequency tracking method was studied to keep the driving frequency consistent with the resonant frequency. The circuit system model of the electrodynamic vibration exciter was built and its impedance characteristics were obtained. It was established that the relationship of between the phase difference and different frequency by simulation. The influence of the output time and stability of the PID parameters were considered, and the parameters were optimal selected, which improved the frequency tracking accuracy of the exciter and speed up the output response speed by 10%.

Keywords. PID, electrodynamic exciter, frequency tracking.

1. Introduction

In the traditional electrodynamic exciter, the working frequency is controlled by the circuit system, and which is generally inconsistent with the resonant frequency according to the working condition. It is difficult for the exciter to output high power [1]. Only when the output frequency of the exciter matches the overall resonant frequency, the conversion of electrodynamic energy from the drive circuit to the vibration mechanical energy of the voice coil motor achieves the highest efficiency and the maximum working amplitude [2-4]. In this paper, the resonance effect was used to improve the output power of the electrodynamic exciter. The diaphragm spring is used as the moving coil of the electrodynamic exciter to improve the overall resonance frequency of the system, and the whole frequency tracking of the whole system of the exciter was carried out to make the output frequency consistent with the resonance frequency.

At present, the phase-locked loop was the commonly used frequency tracking method [5-8]. The tracking range was small and the deadlock phenomenon was easy to occur so that the entire system oscillates. when the system occurs malfunctions, the system needs to be restarted manually to restore the tracking state. And because the resonance point drift is nonlinear, it is difficult to adjust through fixed circuit parameters [9]. Zhai et al. used a method based on the maximum current to search the

[1] Corresponding Author, Wentao Liu, School of Mechanical Engineering, University of Jinan, Jinan 250022, China; E-mail: me_liuwt@ujn.edu.cn

frequency value corresponding to the maximum current. This method was simple, but the frequency tracking accuracy was not high and the stability was poor [10].

This paper using current and voltage phase difference data acquisition and combined with the PID algorithm, the closed-loop control of phase difference was realized. In the PID controller, the input was the error between the setting value and the feedback quantity. The control quantity was calculated by the linear combination of proportional, integral and differential units, and then the actuator was controlled to make the controlled object meet the output requirements.

2. Vibration Exciter

2.1. Mechanical Structure of Vibration Exciter

The structure of the exciter under this research was shown in Figure1, which was composed of a permanent magnet, a movable coil, a transmission support rod, a diaphragm spring and a shell. According to the principle of Ampere force, a constant magnetic field is formed between the permanent magnet and the movable coil. The direction of the force of the charged coil in the magnetic field is a function of the current direction and the magnetic field vector, the polarity of the voltage at both ends of the energized coil determines the direction of the force.

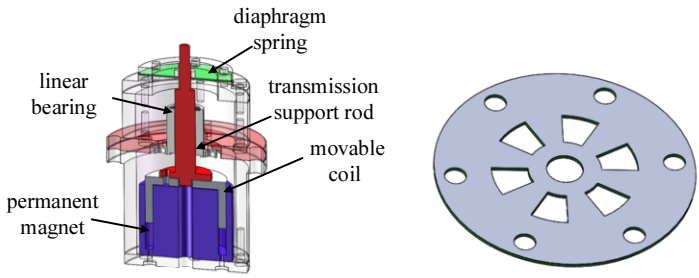

Figure 1. General structure of vibration exciter and diaphragm spring.

2.2. Vibration Impedance Calculation

The driving voltage is u, and the equivalent resistance of the mover coil and the driving circuit is Zc. The input current of the moving coil is I, and the conductor is subjected to magnetic force, which drives the diaphragm spring to move back and forth, and the back electromotive force is generated because the coil will cut the magnetic field movement.

According to Kirchhoff's second law, the algebraic sum of all electromotive forces along the closed loop is equal to the algebraic sum of all voltage drops, and the electric balance equation of the equivalent circuit of the voice coil motor can be obtained. The relationship between the total input voltage of the system u and the equivalent resistance Ra and inductance of the circuit La is as follows:

$$u = e_a + IR_a + L_a \frac{dI}{dt} \tag{1}$$

The motion system composed of moving parts and diaphragm springs can be equivalent to a single-degree-of-freedom vibration system during vibration. The magnetic field force is *F=BIl*, and this system is a forced vibration system. The differential equation of this system is

$$M_m \frac{d^2 x}{dt^2} + C\frac{dx}{dt} + k_s x = F \tag{2}$$

where M_m represents the effective mass of moving parts *kg*, k_s is the dynamic stiffness of the diaphragm spring *N/m*, *C* is the viscous damping coefficient of system structure and material $N \cdot S/m$, X is displacement *m*.

Performing the Laplace transform on the above equation, it can be concluded that $x = F/(M_e s^2 + Cs + k_s)$, and the corresponding speed is *v=sx*. Since the movable coil moves in the magnetic field at this speed, according to Faraday's law of electromagnetic induction, the electromotive force generated at both ends of the excitation coil in the coil is *E=Blv*, and

$$E = \frac{Bl\,s}{M_e s^2 + Cs + k_s} F \tag{3}$$

Because *F=BIl*, the impedance of this counter electromotive force is

$$Z_M = \frac{E}{I} = \frac{(Bl)^2 s}{M_e s^2 + Cs + k_s} \tag{4}$$

Substitute it into the formula s=jω, and the complex form of motion impedance is obtained by

$$Z_M = \frac{(Bl)^2 s}{C + j(M_e\omega - k_s/\omega)} \tag{5}$$

It can be seen that the total impedance of the movable coil is

$$Z_C = Z_E + Z_M = R_a + L_a + \frac{(Bl)^2 s}{C + j(M_e\omega - k_s/\omega)} \tag{6}$$

On account of $R' = (Bl)^2/C$, $C' = M_m/(Bl)^2$, $L' = (Bl)^2/k_s$, the total group resistance expression is

$$Z_C = Z_E + Z_M = R_a + L_a + \frac{(Bl)^2 s}{C + j(M_e\omega - k_s/\omega)} \tag{7}$$

It can be seen from the formula that when the frequency is 0, the overall impedance is equal to the DC resistance of the voice coil motor. As the frequency increasing, the inductance of the driving coil gradually becomes significant. The input impedances are R_a, La and C', therefore, the resonance frequency is

$$f_c = \frac{1}{2\pi\sqrt{L_a C'}} \tag{8}$$

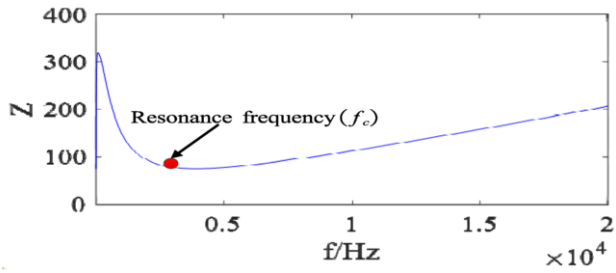

Figure 2. Impedance characteristic curve of the exciter.

Figure 2 shows the variation curve of the exciter impedance with frequency. The minimum impedance point is the resonance frequency. As the dynamic stiffness of the diaphragm spring increasing, the resonant frequency increases, because that La and C' of the Formula (8) were determined by the stiffness of diaphragm spring and the quality of moving parts.

3. Analysis

The transducer frequency tracking model was established by using the Matlab/Simulink program. The purpose was to reflect the working state of the exciter in the actual machining process more intuitively, and provided a reference for the realization of the frequency tracking function. At the same time, the characteristics of the control algorithm was studied.

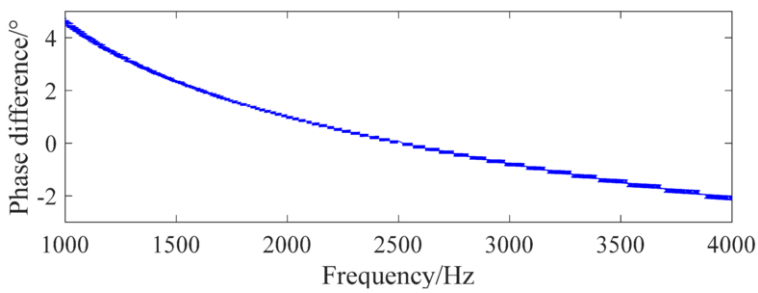

Figure 3. The relationship between frequency and phase difference.

Figure 3 presents the phase differences at different frequencies. It can be seen from the diagram that when the working frequency was greater than the resonant frequency, the voltage was ahead of the current, and when the working frequency of the exciter was less than the resonant frequency, the voltage lagged behind the current. In the

simulation, the positive and negative phase difference represents the lead and lag relationship of the voltage and current phase.

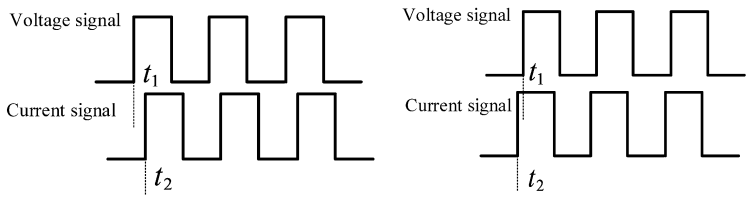

Figure 4. Voltage and current phase waveform diagram.

Figure 4 shows that when the voltage was ahead of the current, the rising edge of the voltage came first, and the time difference was $\triangle t = t_1 - t_2$. When the voltage lags behind the current, the current rising edge came later. By establishing the relationship between time difference, period and phase difference, the phase difference of the system at different frequencies was calculated by

$$Phase\ difference = \frac{\triangle t}{T} \times 360^{\circ} \tag{9}$$

To study the characteristics of the frequency tracking control algorithm, the mathematical model of the electrodynamic exciter should be built. It can be seen from Figure 5 that the system mainly includes four parts: waveform generator module, exciter transfer function module, phase difference detection module and PID controller. To effectively simulate the ultrasonic vibration system and shorten the simulation time, each part was simplified.

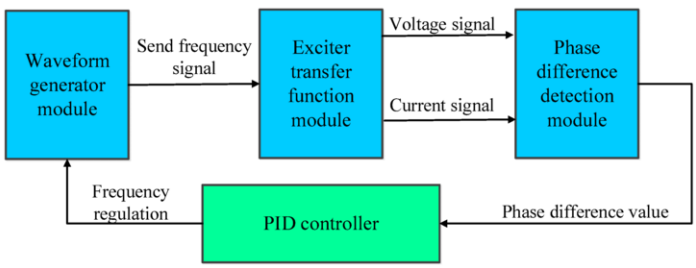

Figure 5. System simulation structure diagram.

The waveform generator module was used to replace the Direct Digital Synthesis (DDS) generator in the actual circuit system, which provides a sinusoidal electrical signal with a certain frequency and a certain voltage for the exciter.

The voltage of the 10 Ω precision sampling resistor was used to reflect the current signal, and the product of the current and the exciter impedance was used as the voltage signal. The input voltage and current were converted into a square wave signal with a duty cycle of 50 % through a zero comparator. The two square wave signals were converted into a phase difference pulse signal by XOR and logic operations. The time difference between the rising edge of each voltage and current square wave was recorded to calculate the phase angle of the phase difference pulse.

The phase difference of different frequencies in the uncontrolled state changes with time as shown in the Figure 6, the time difference corresponded to the initial frequency of 500 Hz was 5.83×10^{-5} s, and the phase difference angle was 10.494° according to Formula (9).

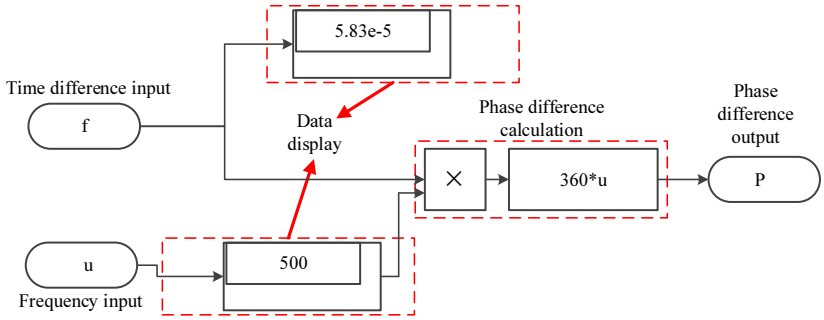

Figure 6. Phase difference calculation module.

According to the impedance analysis results, the impedance characteristic of the transducer was a nonlinear system, which has linear characteristic near the resonant frequency. Because the frequency drift range of the transducer was very small in the actual machining process, the PID control was suitable for tracking the series resonant frequency of the transducer. The working frequency of the transducer was set to 2,500 Hz in PID, and the phase difference of the target input was zero in Figure 7.

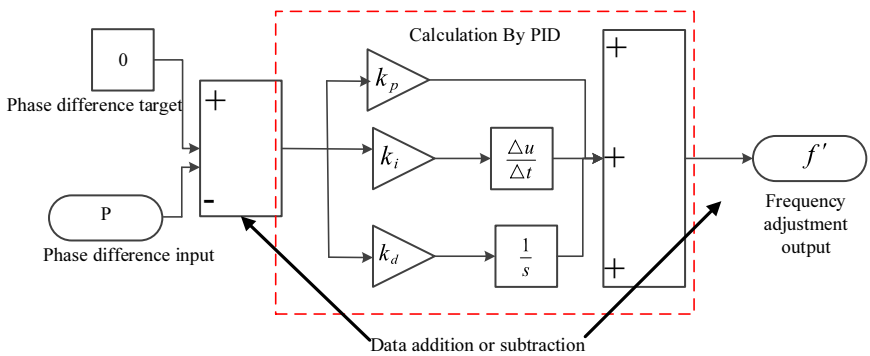

Figure 7. The control module of PID.

It can be seen from Figure 8(a) that the system reached a stable state when the simulation time was 1.26s, and the phase difference remained stable at zero. At this time, the frequency was 2,496 Hz, and the frequency was slightly different from the theoretical value, which was caused by the simplification of the impedance model.

When the value of k_i equals to 1,200, the stable time is 1.26 s, and when the value of ki equals to 1,000, the stable time is 1.87 s. With the increase of k_i, the time of phase difference reaching a stable value become shorter, Figure 9 (a) shows the relationship between the k_i and the time of stabilization, and there was no overshoot when the value was below 1,200. When it exceeds 1,200, excessive integration leads to the decrease of system stability.

Figure 8 (a) and (c) illustrate the frequency change curves with different k_d, Figure 8 (a) and 8 (c) are the frequency-time curves when 0.02 and 0.05, respectively. That fluctuate at 1.8s and 1.71 s, the fluctuation values are around 0.089. It can be seen from Figure 9 (c) that k_d was too large, the corresponding fluctuation of the output increased, the interference signal was amplified, and the vibration process oscillates. If k_d was too small, the transition time of the output response become longer. When the reference value of comprehensive analysis k_d was equal to 0.02, the fluctuation was less and it was suitable for selection.

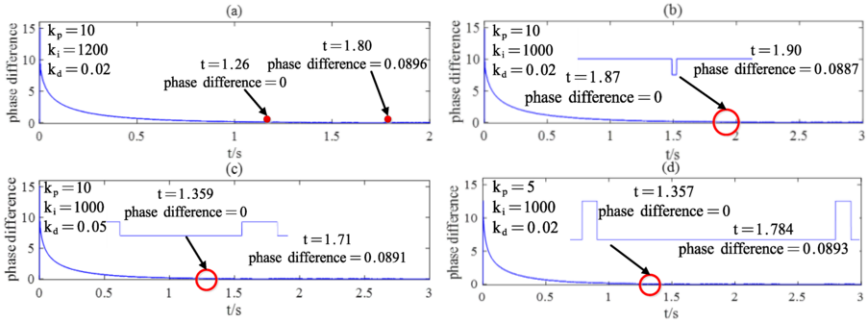

Figure 8. Frequency variation curve under different parameters of PID.

Figure 8 (a) and (d) are the simulation results under different k_p. Figure 8 (a) shows that the control system reached 0.09° at a faster speed, and fluctuated in a stable state. The larger the k_p is, the faster the adjustment speed of the system is, and the error can be quickly reduced as shown in Figure 9 (b). However, when k_p exceeds 10, the phase difference and frequency will oscillate slightly during the adjustment process, which reduces the stability of the system.

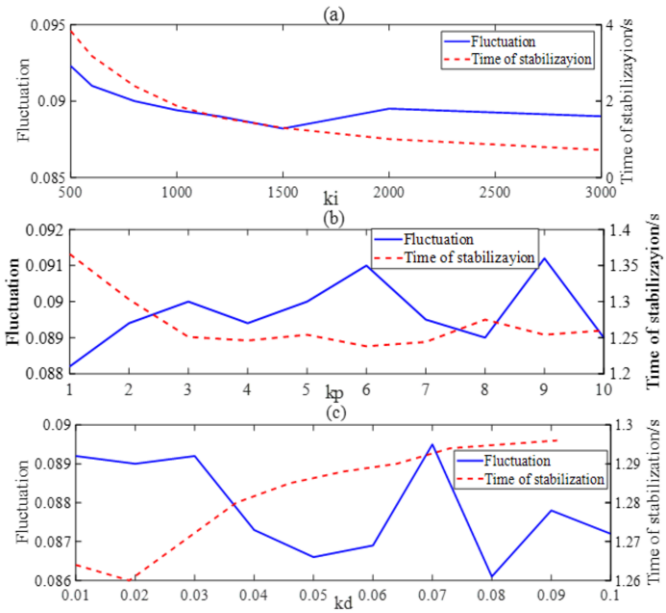

Figure 9. The relationship between parameters of PID, fluctuation and time of stabilization.

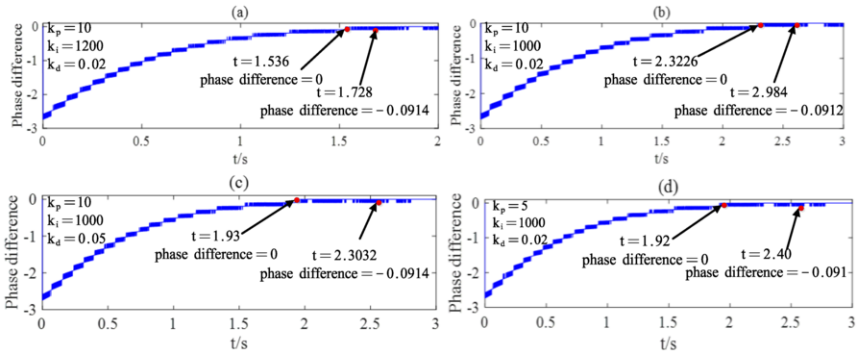

Figure 10. Negative phase difference adjustment.

The adjustment of phase difference from negative to 0° is as plotted in Figure 10, where the initial phase difference was -2.754° at 4,500 Hz. When the frequency exceeds the resonant frequency, the voltage signal was ahead of the current signal, and the phase difference was negative.

Figure 10 (a) shows that after the adjustment of 1.536 s, the stable value was 0, and there are also fluctuations. The fluctuation value was -0.0914°. At this time, the driving frequency was 2,502 Hz, which was consistent with the expected frequency fluctuation.

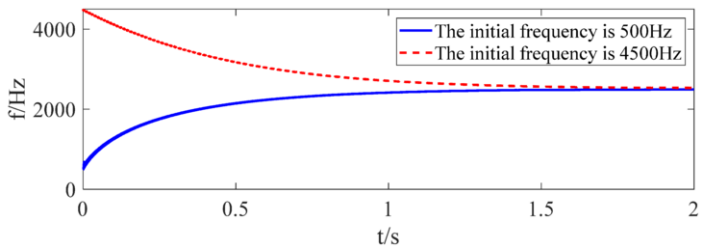

Figure 11. Comparison of frequency adjustment on both sides.

Figure 11 shows two cases of adjusting to the resonant frequency. The initial frequency of blue was less than the resonant frequency, which was adjusted from 500 Hz. The initial frequency of red was 4,500Hz, which was greater than the resonant frequency. The frequency was adjusted close to the resonance point and remains stable after reaching close to 2,500 Hz in both cases.

4. Conclusion

A type of electrodynamic vibration exciter using resonance effect was proposed in this paper. The resonant frequency of the exciter was determined by the stiffness of diaphragm spring and the quality of moving parts. The circuit simulation model of the system was established, and the frequency tracking method in this system was verified, and the relationship between the parameters of the PID and time of stabilization were concluded.

(1) The relationship between different frequency and phase difference of voltage and current is obtained, by means of the simulation without PID control.

(2) It was found that with the increasing of ki and kp, the adjustment time decreased, but the overshoot occurred when ki exceeded 1,200, and there was a large fluctuation when kp was greater than 10. The transition time and fluctuation was determined by the value of kd, and 0.02 was the best choice in the case.

(3) The output frequency was adjusted by controlling the phase difference of voltage and current signals. The algorithm of PID can effectively adjust the phase difference to be zero, regardless of the initial frequency on which side of the resonant frequency.

Acknowledgements

This work was supported by Shandong Innovation Capability Improvement Project of Scientific and Technological Small and Medium-sized Enterprises (2021TSGC1366), Key R&D Plan Projects in Jining City (TQT2301, TQT2302), Shandong Province Bearing Intelligent Manufacturing Innovation and Entrepreneurship Community Project (2021-2023).

References

[1] Long Z, He Y, Li Z, et al. 2016 Dynamic matching model of ultrasonic transducer based on digital inductance. *IEEE*, pp618-625.

[2] Li B, Ding Z. 2012 Research on the frequency automatic tracking in ultrasonic power supply based on fuzzy-DDS.*IEEE*, pp448-451.

[3] Zhou W, Zhang D. 2012 Research and Development of Ultrasonic Frequency Dual Closed-Loop Control Tracking System Based on the STM32 and Phase Inspection Circuit *IEEE*, pp638-641.

[4] Sun C F, Zhang W G. 2012 PWM Chopper of Ultrasonic Power Supply Based on FPGA. *Advanced Materials Research*. pp1305-1308.

[5] Zou P, Xu Y, He Y, et al. 2015 Experimental Investigation of Ultrasonic Vibration Assisted Turning of 304 Austenitic Stainless Steel. *Shock and Vibration*. pp1-19.

[6] Yatsun V, Filimonikhin G, Haleeva A, et al. 2020 Searching for the two frequency motion modes of a three mass vibratory machine with a vibration exciter in the form of a passive auto balancer. *Eastern-European Journal of Enterprise Technologies*. p4(7).

[7] Chandra R T, Sandeep S, Aurobinda R, et al. 2023 Effective fall detection and post-fall breath rate tracking using a low-cost CW Doppler radar sensor. *Computers in biology and medicine*. p164.

[8] Wenzhou L, Xiaoyan Y, Xu X, et al. 2023 Improved climbing algorithm with variable step size in tidal energy Application of maximum power tracking control technique for power generation system. *Journal of Physics: Conference Series*, p2495(1).

[9] Pramod K, Ashish S. 2023 Maximum power tracking from solar PV system by using fuzzy-logic and incremental conductance techniques. *Materials Today: Proceedings,* p79(P2).

[10] Zhiyong G, Lihong Z. 2022 Research on ultrasonic cleaning power frequency tracking technology based on fuzzy adaptive PID. *Journal of Physics: Conference Series*, p2383(1).